First-Principles Calculations of the Specific-Heat Mass Enhancements in UIr_3, UPt_3, and UAu_3

M. M. Steiner,[1,2,3] R. C. Albers,[1] and L. J. Sham[2]
[1] *Theoretical Division, Los Alamos National Laboratory, Los Alamos, New Mexico 87545*
[2] *Department of Physics, University of California at San Diego, La Jolla, California 92093-0319*
[3] *Department of Physics, Ohio State University, Columbus, Ohio 43210-1106*
(Received 13 December 1993)

By including dynamic fluctuations around the local-density-approximation (LDA) electronic structure we find good agreement for the specific-heat mass-enhancement factors for UX_3 (X =Ir, Pt, Au). The fluctuations, which are calculated through to second order in the perturbation, are restricted to those caused by strong, local, uranium $5f$ electron-electron interactions, for which the calculated effective interaction strength is 2 eV. The strong material dependence of the second-order mass-enhancement factors is related to the composition dependence of the Fermi energy and the underlying one-electron LDA density of states.

PACS numbers: 71.28.+d, 65.40.Em, 71.45.Gm

A large amount of work on the heavy-fermion systems has established their essential strong-interaction nature [1]. We wish to address a different question: what makes a particular system heavy fermionic? An example is the $5d$-metal dependence of the low-temperature linear coefficient of the specific heat, $\gamma^{\rm exp}$, for UX_3 (X =Ir, Pt, Au) (see row 1 of Table I). In complex systems, theoretical predictions of such material dependencies are faced with the difficult task of adequately treating both one-electron and correlation effects. Consequently, approximations must be made, and a central issue becomes the relative importance of the two sets of effects. Generally, model many-body calculations simplify the one-electron term and then treat the correlation effects as well as possible, while techniques based on density-functional theory account well for the one-electron effects, such as hybridization and the separation of levels, but treat the exchange and correlation term in the local-density approximation (LDA). Although the LDA approach has successfully accounted for ground-state properties, the common use of LDA single-particle orbitals for excited states misses important correlation effects, particularly for strongly correlated electron systems. Indeed, by comparing rows 1 and 2 in Table I we see that the LDA does not reproduce the experimental trend of the low-temperature specific heat. Our calculations are an attempt to extend the range of applicability of LDA-based approaches to properties and systems where the dynamics of localized electrons are important. The success of the method is illustrated in row 3 of Table I, which shows that our approach gives a good account of the specific-heat variation. That is, we find that UIr_3 is only slightly enhanced with respect to the LDA results, while UPt_3 is strongly enhanced, and "UAu_3" [2] lies somewhere in between. Below, we give our understanding of the physical factors driving this material dependence.

TABLE I. Comparison of experimental, $\gamma^{\rm expt}$ [7], LDA, $N^{\rm LDA}(E_F)$, and our results, $\gamma^{(2)}$, for the effective masses of UIr_3, UPt_3, and UAu_3. Using the calculated (material-independent) estimate for the effective electron-electron interaction strength of 2 eV, we obtain results which are in fair agreement with experiment, showing the ability of our second-order approach to determine the low-energy excitations of these systems. All entries given in mJ K^{-2}/(mol of U).

	UIr_3	UPt_3	"UAu_3"
$\gamma^{\rm expt}$	19.5	452	260
$N^{\rm LDA}(E_F)$	13.1	25.9	28.1
$\gamma^{(2)}$	17	475	243

Before presenting our approach we briefly summarize the LDA electronic structure. Figure 1 shows the total and the partial U-$5f$ density of states (DOS) of UPt_3,

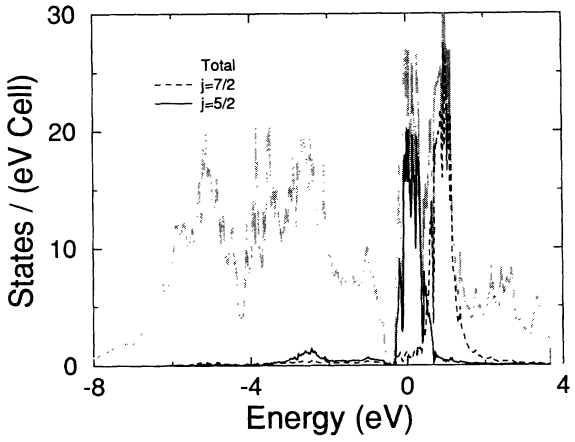

FIG. 1. The total and U-$5f$ relativistic LDA DOS for UPt_3. The spin-orbit split U-$5f$ states have been j resolved. The double peak structures centered around -4 eV are the spin-orbit split Pt-$5d$ states, which are found to be in good agreement with x-ray photoelectron results in contrast to the localized U-$5f$ states. The Fermi energy is at zero energy.

0031-9007/94/72(18)/2923(4)$06.00

computed within the LDA. XPS measurements show the Pt-5d states form a broad peak at 4 eV below the Fermi energy, consistent with the LDA, indicating that the LDA correctly describes the conduction states [3]. Figure 1 also shows the U-5f states, which are pinned to the Fermi energy by the high degeneracy of the f bands and Coulombic considerations, are split by the relativistic spin-orbit coupling term of about 1 eV. They are broadened through hybridization, principally with the Pt-6p and Pt-5d states [4]. The Fermi energy lies in the middle of the lower of the two resulting subbands, producing a complex Fermi surface, which shows agreement with de Haas van–Alphen experiments that is comparable to that found in the noble metals [5,6]. Even though the U-5$f_{5/2}$ LDA bands have the right shape and are narrow (~ 0.8 eV wide), the LDA-DOS at the Fermi energy, $N^{\mathrm{LDA}}(E_F)$, is a factor of 18 smaller than the measured linear coefficient of the low-temperature specific heat, γ^{expt} (see Table I).

The presence of quasiparticlelike excitations can be inferred from experiment, e.g., the linear term in the specific heat and the Pauli-like magnetic susceptibility, along with the agreement between the LDA results and de Haas–van Alphen experiments. This strongly supports a Fermi liquid interpretation of the low-temperature properties, and indicates the possible fruitfulness of a perturbative approach for getting from the unperturbed, uncorrelated state to the low-temperature Fermi-liquid state.

Our approach is similar to the one used earlier for the 3d ferromagnets [8] and the periodic Anderson model [9]. We assume that the LDA provides an adequate description of all non-U-5f states. However, as the U-5f orbitals are localized, we expect electrons in these orbitals to experience a strong, Hubbard-type, on site, *effective* electron-electron interaction, U. Although the time-averaged (or mean-field) contribution of this interaction is accounted for by the LDA, important *dynamic* correlations are left out. We correct for this neglect by perturbatively including fluctuations *around* the LDA results to lowest nonvanishing order in U (i.e., second order).

Since the Hubbard U is a local property that should not depend too much on the environment surrounding the uranium atoms, we used the same calculated value of $U = 2$ eV for all three compounds [10].

The complexity of the UX_3 materials prohibits us from calculating the self-energy of the U-5f bands as completely as we have for other systems. In the 3d ferromagnets we found that the momentum ($\mathbf{k}$) dependence of the self-energy is weak because of the many ways of simultaneously conserving energy and momentum in a multiband system [8]. In UPt_3 even more bands cross the Fermi energy, leading to an even weaker $\mathbf{k}$ dependence for the self-energy, which we have consequently neglected. Figure 1 shows that the U-5$f_{5/2}$ and U-5$f_{7/2}$ states are well separated, and so the self-energy will depend strongly on the relativistic quantum number j. On the other hand, the dependence on the relativistic azimuthal quantum number m_j is much weaker, due to Brillouin zone averaging. Therefore we assumed that the partial DOS depends on j, but not on m_j. Although it would be desirable to study the stability of heavy-fermion systems with respect to magnetic instabilities, we have not done so because of the greatly added computational effort. However, we note that, both for model systems and the 3d ferromagnets, the tendency towards magnetism is reduced by correlation effects [8,11].

Figure 2 shows the imaginary part of the j-resolved, second-order self-energies, $\mathrm{Im}\{\Sigma_j^{(2)}(\omega)\}$, for the U-5$f$ states in UPt_3. The main features can be understood: the peaks labeled A, B, and C correspond to virtual $j = 5/2$ electron-hole pairs being created by $j = 7/2$ electrons, $j = 5/2$ electrons, and $j = 5/2$ holes, respectively. The rapid rise of the $j = 5/2$ term on each side of the Fermi energy (lying between B and C) reflects the large $j = 5/2$ DOS into which the electrons and holes can scatter. This is in contrast to the $j = 7/2$ channel near the Fermi energy, which has a DOS almost a factor of 20 lower. The large scattering rate of $j = 5/2$ states leads to a correspondingly large mass-enhancement factor.

The mass enhancement factor, $1 - \frac{\partial \mathrm{Re}\{\Sigma_j(\omega)\}}{\partial \omega}|_{\omega=\mu}$, can be derived from the Kramers-Kronig relationship:

$$\left.\frac{\partial \mathrm{Re}\{\Sigma_j(\omega)\}}{\partial \omega}\right|_{\omega=\mu} = \frac{1}{\pi}\int d\omega' \frac{\mathrm{Im}\{\Sigma_j(\omega')\}}{(\omega'-\mu)^2}. \qquad (1)$$

The $(\omega'-\mu)^{-2}$ factor strongly weights the region near the Fermi energy. An analysis of the integral shows that the region 0.1 eV on each side of the Fermi energy accounts for nearly half of the $j = 5/2$ states enhancement, a point we return to.

The strong material dependence of the mass-enhancement factors for the $j = 5/2$ states for the three materials is shown in row 1 of Table II. However, comparison with the ratio of the experimental results to the LDA

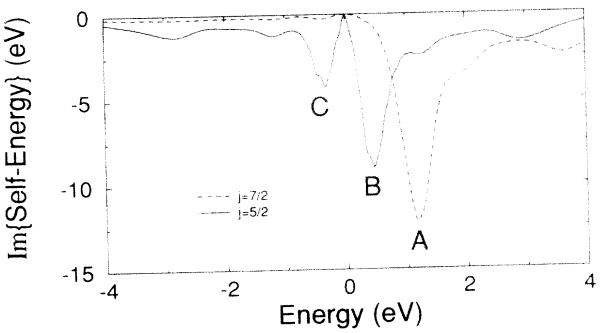

FIG. 2. The imaginary part of the U-5f j-resolved second-order self-energies for UPt_3. The features labeled A, B, and C arise from $j = 5/2$ electron-hole pairs being created by the scattering of a $j = 7/2$ electron, a $j = 5/2$ electron, and a $j = 5/2$ hole, respectively. The large curvature of the $j = 5/2$ term gives rise to a large mass-enhancement factor for $j = 5/2$ states. The Fermi energy is at zero energy.

TABLE II. For UIr_3, UPt_3, and "UAu_3" we compare the second-order prediction for $j = 5/2$ mass-enhancement factor, $1 - \partial \mathrm{Re}\{\Sigma^{(2)}_{5/2}(\omega)\}/\partial\omega|_{\omega=\mu}$, with the ratio of the experimental specific heat to the LDA mass, $\gamma^{\mathrm{expt}}/N^{\mathrm{LDA}}(E_F)$. There is approximately a factor of 2 between the two numbers, reflecting the fact that not all of the states at the Fermi energy are $j = 5/2$ states. We also compare the two with the average $j = 5/2$ DOS near the Fermi energy, $\tilde{N}^{\mathrm{LDA}}_{5/2}(E_F)$. The correlation of this one-electron property further illustrates the important role of the underlying band structure in determining the low-energy excitations of the system. DOS are given in mJ K^{-2}/(mol of U) .

	UIr_3	UPt_3	"UAu_3"
$1 - \left.\frac{\partial \mathrm{Re}\{\Sigma^{(2)}_{5/2}(\omega)\}}{\partial\omega}\right\|_{\omega=\mu}$	2	31	17
$\frac{\gamma^{\mathrm{expt}}}{N^{\mathrm{LDA}}(E_F)}$	1.5	17.5	9.2
$\tilde{N}^{\mathrm{LDA}}_{5/2}(E_F)$	2.6	21.1	15.1

results (see row 2) shows that the $j = 5/2$ enhancement is approximately 2 times too large. The reason is that not all the states at the Fermi energy experience this enhancement. (The $j = 7/2$ enhancement factors are small, and the remaining states, e.g., Pt-5d and Pt-6p, are not directly enhanced). This variation in the enhancement for different states is supported by de Haas–van Alphen experiments, which show that some of the bands are only weakly enhanced with respect to the LDA predictions. In order to account for such variable enhancements both one-electron effects and correlation effects need to be included when computing the quasiparticle bands. This is done by solving the modified Dyson equation

$$G_{\mathbf{k}}(\omega) = G^{\mathrm{LDA}}_{\mathbf{k}}(\omega) + G^{\mathrm{LDA}}_{\mathbf{k}}(\omega)\, \tilde{\Sigma}^{(2)}(\omega)\, G_{\mathbf{k}}(\omega)\ , \qquad (2)$$

where the one-electron effects, such as hybridization and energy splittings, are included in the LDA Green's function $G^{\mathrm{LDA}}_{\mathbf{k}}(\omega)$, and the correlation effects are accounted for in the energy-dependent self-energy. The modification $\tilde{\Sigma}^{(2)}(\omega) \equiv \Sigma^{(2)}(\omega) - \Sigma^{(2)}(\mu)$ would be correct if the LDA Green's function were replaced by the full density functional Green's function [12]. The resulting quasiparticle peaks along high symmetry directions show that near the Fermi energy some of the bands are strongly enhanced, while others remain similar to the LDA bands.

In our discussion of Fig. 2 we mentioned that the $j = 5/2$ DOS near the Fermi energy leads to the large enhancement factor for these states. In row 3 of Table II we give the U-5f $j = 5/2$ DOS averaged over a region 0.1 eV on each side of the Fermi energy, $\tilde{N}^{\mathrm{LDA}}_j(E_F)$. For a simple half-filled one-band system with a rectangular DOS one finds near the Fermi energy $\mathrm{Im}\{\Sigma^{(2)}(\omega)\} \propto \omega^2 N^{\mathrm{LDA}}(E_F)^3$ (essentially one factor for each propagator). Even though one does not find a cubic relation for more complex systems, a comparison of rows 1 and 3 of Table II shows a correlation between the enhancement factor and $\tilde{N}^{\mathrm{LDA}}_j(E_F)$.

The material dependence of $\tilde{N}^{\mathrm{LDA}}_j(E_F)$ can be understood. The effective nuclear charge of the 5d metal increases from Ir to Au, causing the 5d bands to move away from the U-5f level. Consequently the smaller degree of mixing between the U-5f and the 5d states in UAu_3 than in UIr_3 causes the U-5f bands to become narrower and have less conduction state character [13]. Concomitantly, the number of electrons per unit cell increases by 3, shifting the Fermi energy from the bottom of the U-$5f_{5/2}$ peak in UIr_3 to the middle in UPt_3, and then to near the top in "UAu_3." Because of Coulombic considerations the overall result of changing the relative position of the Fermi energy and redistributing the U-5f DOS does not much affect the total number of U-5f electrons (2.48, 2.74, and 2.65, respectively). On the other hand, the weight in the U-5f tails in the 5d-band region drops dramatically from 2.25 to 1.53 to 0.59, illustrating the redistribution of the U-5f weight. The fact that the total U-5f occupation hardly changes indicates that the LDA can capture the fact that it is energetically unfavorable to change the U-5f occupation too much, and so provides *a posteriori* support for our setting the LDA result equal to the mean-field solution about which we perturb.

The agreement between experiment and our specific-heat results and our tracing the material dependence of the enhancement back to the underlying one-electron band structure lead to the question: How general is the correlation between $\tilde{N}^{\mathrm{LDA}}_{5/2}(E_F)$ and the mass-enhancement factor? We found that, although there is no overall correlation between the different types of strongly enhanced materials, in small groups of materials the enhancement factors correlate with the $\tilde{N}^{\mathrm{LDA}}_{5/2}(E_F)$. In these comparisons it is important to remember that only the U-5f DOS are enhanced [14]. A typical example is the substitution of Pd for Rh in URh_3. The Fermi energy moves from the bottom (low DOS) of the U-$5f_{5/2}$ peak into the middle (high DOS), and results in a large increase in the enhancement factor, driving the system towards the localized limit [15]. Another example is the series UIr_2, $NpIr_2$, and $PuIr_2$. If we suppress the antiferromagnetic transition in $NpIr_2$, we find that $\tilde{N}^{\mathrm{LDA}}_{5/2}(E_F)$ and the mass enhancement increase on going from the UIr_2 to $NpIr_2$ [16]. Although the $PuIr_2$ specific heat has not been measured, we expect it to be comparable to (or maybe slightly lower than) that of the Np compound.

We now address a few additional points. First, as mentioned above, a 0.1 eV energy range around the Fermi energy accounts for more than half the enhancement. While this is smaller than the relevant bandwidth (0.8 eV), it is large compared to the relevant low-temperature scales of the problem, so we must worry about higher-order terms. Even though Luttinger showed that the second-order contribution to the imaginary part of the self-energy near the Fermi energy dominates any other order

[17], the summation of an infinite series (i.e., the T matrix) might produce large renormalization effects. Early work based on free-electron ferromagnetic paramagnons [18] can explain the temperature dependence of the specific heat, but is unable to explain the type of trend found on going from UIr_3 to UAu_3. Later work by Norman [19] found good agreement for the temperature dependence of the specific heat, but required knowledge of the experimental susceptibility. Second, it is fortuitous that the value of U suggested by Herbst *et al.* [10] gives such good agreement, especially since we could not use the values of U obtained by similar constrained density-functional-theory calculations for the $3d$ transition metals [8], which have about the same radial extension. Third, one would naively expect higher-order terms to change the mass enhancement and worsen the agreement with experiment. However, on including higher-order terms the value of the *effective* interaction U should also change, to avoid double counting screening effects already in U. For example, Bulut and Scalapino [20] found that the effective interaction needed for RPA susceptibility calculations to reproduce Monte Carlo results is half the value used in the Monte Carlo calculations. Finally, with respect to energies away from the Fermi energy, joint x-ray photoelectron and bremsstrahlung isochromat spectra show a 4–5 eV wide peak around the Fermi energy [21]. We find that much of the U-5f spectral density is shifted to 4–6 eV above the Fermi energy, because the $\mathrm{Re}\Sigma^{(2)}(\omega)$ deviates strongly from the expected limiting atomic type of behavior $\Sigma(\omega) \sim U^2/4\omega$ at high energies [12,22].

To conclude, we found good agreement with experiment for the specific heat of UX_3 (X = Ir,Pt,Au). By tracing the origin of the material dependence of the mass enhancement back to changes in the one-electron band structure we showed that, despite the importance of many-body effects, properties of heavy-fermion systems can depend crucially on the underlying material-specific one-electron spectrum, which is well described by the LDA. More specifically, the enhancement factor correlates well with the average LDA U-5$f_{5/2}$ DOS in the vicinity of the Fermi energy, which is dependent on the chemical composition through the filling, the hybridization, and the on-site energies of the components.

M.M.S. was supported by the University of California's INCOR superconductivity program, with additional support from DOE–BES–DMR. He wishes to thank O. Eriksson, M. Alouani, K. Yonemitsu, and J. Wilkins for many useful discussions. L.J.S. acknowledges partial support by the NSF under Grant No. DMR-91-17298 and by the CMS, LANL. We acknowledge the essential supercomputing time provided by the DOE.

[1] H. R. Ott, in *Progress in Low Temperature Physics*, edited by D. F. Brewer (Elsevier Science Publishers, Amsterdam, 1987), Vol. XI; P. A. Lee *et al.*, Comments Condens. Matter Phys. **12**, 99 (1986); P. Fulde, J. Keller, and G. Zwicknagl, Solid State Phys. **41**, 2 (1988); N. Grewe and F. Steglich, in *Handbook on the Physics and Chemistry of Rare Earths*, edited by K. A. Geschneidner and L. Eyring (Elsevier, Amsterdam, 1991), Vol. 14, p. 345.

[2] A. Dommann and F. Hulliger, J. Less-Common Met. **141**, 261 (1988).

[3] P. Marksteiner *et al.*, Phys. Rev. B **34**, 6730 (1986).

[4] R. C. Albers, Phys. Rev. B **32**, 7646 (1985).

[5] M. R. Norman *et al.*, Solid State Commun. **68**, 245 (1988); C. S. Wang *et al.*, Phys. Rev. B **35**, 7260 (1987).

[6] N. E. Christensen *et al.*, J. Magn. Magn. Mater. **76 & 77**, 23 (1988).

[7] M. Brodsky *et al.*, in *Magnetism and Magnetic Materials—Philadelphia, 1975*, edited by J. Becker *et al.*, AIP Conf. Proc. No. 29 (AIP, New York, 1976), p. 317; G. R. Stewart *et al.*, Phys. Rev. Lett. **52**, 679 (1984); G. R. Stewart, Rev. Mod. Phys. **56**, 755 (1984).

[8] M. M. Steiner, R. C. Albers, and L. J. Sham, Phys. Rev. B **45**, 13 272 (1992).

[9] M. M. Steiner *et al.*, Phys. Rev. B **43**, 1637 (1991).

[10] J. Herbst, R. Watson, and I. Lindgren, Phys. Rev. B **14**, 3265 (1976); M. Brooks *et al.*, Physica (Amsterdam) **144B**, 1 (1986).

[11] M. M. Steiner, R. C. Albers, and L. J. Sham (unpublished).

[12] It will be shown elsewhere that the second-order self-energy is not correct at high energies in degenerate systems, but simple modifications (based on a moment expansion) can fix it up, resulting in a more symmetric $\mathrm{Im}\{\Sigma(\omega)\}$, which simultaneously improves agreement with XPS data and dramatically reduces $\mathrm{Re}\{\Sigma^{(2)}(\mu)\}$, without changing the low-energy properties.

[13] R. C. Albers, A. M. Boring, and N. E. Christensen, Phys. Rev. B **33**, 8116 (1986).

[14] The DOS from a *relativistic* calculation must be used, as the reduction in degeneracy by the spin-orbit splitting of 1 eV strongly influences the position of the Fermi energy.

[15] O. Eriksson *et al.*, Phys. Rev. B **38**, 12 858 (1988), and references therein.

[16] O. Eriksson *et al.*, Phys. Rev. B **39**, 5647 (1989), and references therein.

[17] J. M. Luttinger, Phys. Rev. **121**, 942 (1960).

[18] S. Doniach and S. Engelsberg, Phys. Rev. Lett. **17**, 750 (1966).

[19] M. R. Norman, Phys. Rev. Lett. **59**, 232 (1987); Phys. Rev. B **37**, 4987 (1988).

[20] N. Bulut and D. J. Scalapino, Phys. Rev. Lett. **67**, 2899 (1991).

[21] J. W. Allen *et al.*, Phys. Rev. Lett. **54**, 2635 (1985).

[22] J. Hubbard, Proc. R. Soc. London A **276**, 238 (1963); **277**, 237 (1963) (for the degenerate atomic limit.)